

# Formwork Fabrication Freedom for a Concrete Canoe

## Journal Article

### Author(s):

Jipa, Andrei ; Bernhard, Mathias ; Ruffray, Nicolas; Wangler, Timothy; Flatt, Robert J. ; Dillenburger, Benjamin 

### Publication date:

2019-09-06

### Permanent link:

<https://doi.org/10.3929/ethz-b-000387459>

### Rights / license:

[Creative Commons Attribution-NonCommercial-NoDerivatives 4.0 International](#)

### Originally published in:

Gestão & Tecnologia de Projetos 14(1), <https://doi.org/10.11606/gtp.v14i1.148264>

# FORMWORK FABRICATION FREEDOM FOR A CONCRETE CANOE

ARTIGO

Andrei Jipa<sup>1</sup>, Mathias Bernhard<sup>1</sup>, Nicolas Ruffray<sup>2</sup>, Timothy Wangler<sup>2</sup>, Robert Flatt<sup>2</sup>, Benjamin Dillenburger<sup>1</sup>

**ABSTRACT:** The pursuit for complex geometries in contemporary architecture is driving innovation towards an unconstrained fabrication freedom for building components. Concrete is a building material with excellent structural and architectural qualities, which has the theoretical capacity of being cast into any shape. However, in practice, concrete is generally limited by the formwork manufacturing industry to solid, planar shapes. The aim of this research is to overcome the fabrication limitations for formwork and, indirectly, for concrete. To achieve this aim, the objective of this research is twofold: a) enable the fabrication of building-scale concrete components through 3D-printed plastic formworks and b) develop computational design and optimisation methods suitable for this fabrication method. The resulting design and construction method takes advantage of the load-bearing capacity of concrete and relies on the fabrication freedom inherited from the 3D-printed formwork, thus making complex topologies and precise details possible for concrete structures. The research method for demonstrating this fabrication process focused on the design to fabrication steps of skelETHon —a functional four-meter-long concrete canoe— which was designed, built and raced in a regatta on the Rhine river (Figure 1). The main research achievement was the fabrication of the canoe, an optimised truss-like concrete component with members as thin as 15 mm in diameter. Such slender geometric features are difficult to produce in concrete with other known formwork systems.

<sup>1</sup> Digital Building Technologies, ITA, D-Arch, ETH Zürich

<sup>2</sup> Physical Chemistry of Building Materials, IfB, D-Baug, ETH Zürich

**KEYWORDS:** Concrete; 3D Printing; Formwork; Topology Optimisation; Canoe.

## How to cite this article:

JIPA, A.; BERNHARD, M.; RUFFRAY, N.; WANGLER, T.; FLATT, R.; DILLENBURGER, B. Formwork Fabrication Freedom for a Concrete Canoe. *Gestão e Tecnologia de Projetos*, São Carlos, v.14, n.1, p.25-44, set.2019. <http://dx.doi.org/10.11606/gtp.v14i1.148264>

## Fonte de financiamento:

Declaro não haver

## Conflito de interesse:

Declaro não haver

**Submetido em:** 17/07/2018

**Aceito em:** 21/02/2019





**Figure 1:** skeETHon, the four-metre-long canoe made entirely out of concrete.

**Source:** DBT, ETH Zürich, 2017

## INTRODUCTION

With serious concerns regarding the vulnerable state of the environment, material efficiency is becoming a critical design driver in architecture. This is especially relevant for materials that are difficult to recycle, such as concrete. Concrete is of particular relevance in relation to material efficiency because it is by far the most used construction material in the world, being used twice as much as all the other construction materials combined (Crow, 2008). Moreover, the amount of concrete used annually is predicted to double in the next thirty years.

Concrete is used in such vast amounts for good reasons. Its excellent structural properties, combined with its versatility, make concrete indispensable in a wide variety of environments and applications, both for buildings and infrastructure works. Furthermore, concrete is celebrated by architects because it can be cast into any shape and thus it is in theory capable of materialising almost any imaginable design.

But this formal flexibility has applications beyond architectural aesthetics. The recent rise in computational form-finding tools such as topology optimisation has demonstrated how considerable material savings can be achieved by manipulating the geometry of structures and distributing material precisely where it is most needed, without affecting, or sometimes even improving the overall performance and functionality. Designing with material efficiency as a goal can be achieved through ribbings, porosity gradients, hierarchical articulations, venations and other similar geometric features (Amir, 2013; Jipa et al, 2016).

Given the significant amount of concrete used around the world, optimising concrete structures for reducing material use can have a global impact in releasing pressure from natural resources and reducing the carbon footprint of buildings and infrastructure. However, this excellent potential of concrete is only enabled by complex optimised shapes, and achieving such shapes is in turn limited by the capacity to fabricate the necessary formwork.

### Formwork

“...although reinforced concrete has been used for over a hundred years and with increasing interest during the last decades, few of its properties and potentialities have been fully exploited so far. Apart from the unconquerable inertia of our own minds, which do not seem to be able to adopt freely any new ideas, the main cause of this delay is a trivial technicality: the need to prepare wooden frames.”

(Nervi, 1956, p. 56)

This paper describes a method that aims to overcome the limitations of the traditional wooden formwork described by Nervi and unlock the full geometric potential of concrete.

In order to relinquish concrete from the orthogonal constraints of the flat mould panel, new types of formwork with less geometric limitations are needed. New, free-form formwork systems can expand the geometric freedom available for concrete components. Such non-standard shapes can reduce material use in large-scale, functional, load-bearing structures by mass customising concrete components for their specific context, boundary conditions and load-cases.

Aside from its key role in defining the shape of concrete structures, formwork is also a critical topic in concrete construction because it accounts for roughly 50% of the overall costs —more than the costs of cementitious materials, aggregates, additives, reinforcement and labour combined (Robert, 2007). For one-of-a-kind, non-standard shapes, the costs of formwork can be even more significant (Figure 2).

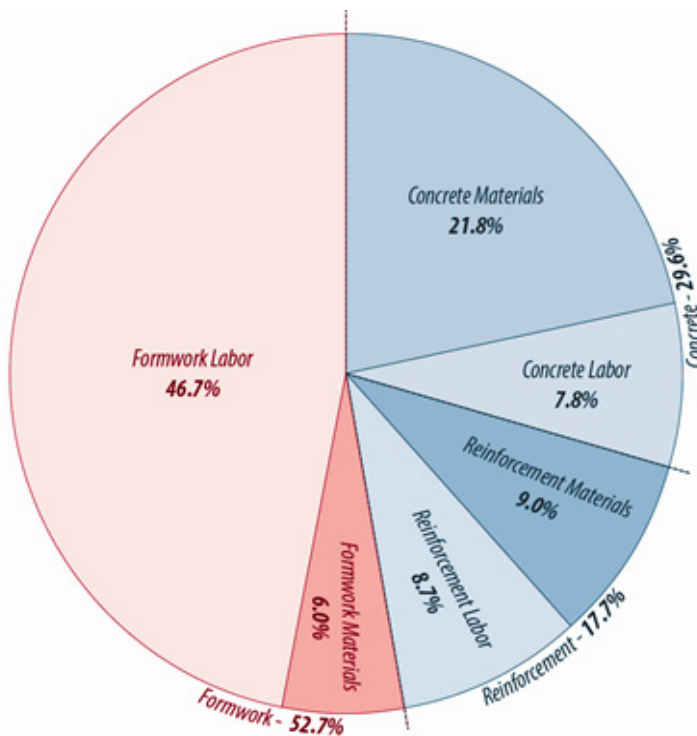


**Figure 2:** The average distribution of costs for concrete constructions. Formwork raw materials and labour are responsible for roughly half the overall costs. This figure highlights the importance of optimising formwork fabrication processes.

**Source:** DBT, ETH Zürich, 2017

## Related works

Architects designing topologically complex concrete elements with material economy in mind are therefore facing the limitations of the available formwork fabrication methods. A compromise has to be made between material efficiency and formwork fabrication costs.

To aid in this dilemma, digital fabrication of formwork is already being investigated. Production of formwork for non-standard concrete elements can be done by CNC milling of foam blocks (Søndergaard & Dombernowsky, 2011), CNC milling of wax (Gardiner & Janssen, 2014), actuated moulds (Oesterle et al., 2012), robotic extrusion (Hack et al., 2013), robotic hot wire cutting (Rust et al., 2016), laser-cutting and folding polypropylene sheets (Kaczynski, 2013) or robotic welding (Hack & Lauer, 2014). Certain types of lightweight formwork can also be produced with patterning fabric (Veenendaal et al., 2011) or with knitting (Popescu et al., 2018). However, all these approaches are resource-intensive as regards the necessary time and labour (robotic cutting and milling tools are slow and wasteful processes,

while fabrics require extensive patterning) and have limitations regarding the geometries that can be produced (e.g. no undercuts for milling, provision for collision-free robotic tool-head access paths, only ruled surfaces for wire-cutting and only smooth anticlastic surfaces for fabrics).

### Objectives. 3D-Printed Formwork

To overcome these limitations, different 3D printing technologies have already been proposed for formwork, such as binder jetting of sand (Morel & Schwartz, 2015; Aghaei-Meibodi et al., 2017). Binder jetting is particularly interesting because of its precision, great level of geometric flexibility and availability in large scale. Still, certain geometric features, such as long tubular voids are difficult to achieve because of the necessary post-processing steps, such as unbonded sand removal and surface infiltration for stability. Moreover, due to the frail nature of the 3D prints, very thin free-standing features, such as millimetre-thick shells are also a challenge.

Another 3D printing technology, fused deposition modelling (FDM) has also been proposed for fabricating formwork (Peters, 2014; Jipa et al., 2017). However, there are some inherent characteristics of FDM 3D printing that need to be addressed in order to make it feasible for large scale fabrication.

This research builds up on the state-of-the-art of 3D-printed formwork, targeting the fabrication of building-scale elements. In particular, the research is addressing the following two-fold research objectives and questions:

a) Develop an efficient fabrication process for free-form concrete components based on 3D printing. To address this objective, how to optimise the 3D printing process? and how to stabilise the plastic formwork during casting? are critical research questions.

b) Develop associated computational design and optimisation processes which synergise with the free-form capabilities of the 3D printing fabrication process. The associated research questions are: what is the design potential for new concrete components? and what are the advantages of the new components beyond aesthetics (e.g. material reduction, structural optimization etc.).

## METHODOLOGY

To pursue the objectives stated in the previous section, the methodology follows the design and fabrication process of a four-meter-long functional concrete canoe, dubbed *skeLETHon* (Figure 1) due to the resemblance of its structural system with a biological skeleton. The canoe demonstrates how even for complex load-cases, computational optimisation can facilitate material reduction and effectively enable a concrete boat to be light enough to float and support two people. The main design to fabrication steps are covered in this chapter: the computational design (Section 2.2), the shape optimisation (Sections 2.3), the 3D printing of the Formwork (Section 2.4 and 2.5), the concrete casting and the formwork removal (Section 2.6).

### Why a concrete canoe?

At a first glance, a concrete canoe is a counter-intuitive challenge and may seem a parody project of sorts, akin a steel plane. Nonetheless, concrete canoe competitions have a long-standing tradition, having been organised in the US since the 1960s. They are currently a well-respected international phenomenon, attracting crowds of hundreds of participants at annual or biennial regatta events organised in more than 20 countries around the world.

*skeLETHon* took part in the 16th Concrete Canoe Regatta in June 2017 in

Cologne, Germany. Approximately 1`000 participants registered 90 concrete boats and raced them for 200 metres at a flat-water racing facility on the Rhine river. This particular race route included two 100-metre-long straight lines where the hydrodynamic designs could demonstrate their top-speeds, as well as a 180o turn to prove the stability of the boats and cornering skills of the competitors. The German Regatta is an important event, with Lafarge-Holcim and Sika being among the sponsors. While also a sporting event, it mainly draws scientific interest for demonstrating innovations in concrete construction methods. The canoe regattas in Germany have been over the years stepping stones for research projects which have since become valuable contributions to the scientific community, like Mesh Mould (Hack & Lauer, 2014) and Smart Dynamic Casting (Lloret et al., 2015).

Apart from a similar scale to building components, a canoe has complex load-cases, which make it a representative case-study for architecture. The canoe has to be designed for the floating load-case in water (self-weight, live point loads from two canoeists ( $P_1$ ,  $P_2$ ), and a distributed support force provided by the hydrostatic pressure) as well as for a transport load-case on land (two support points and self-weight) (Figure 3).

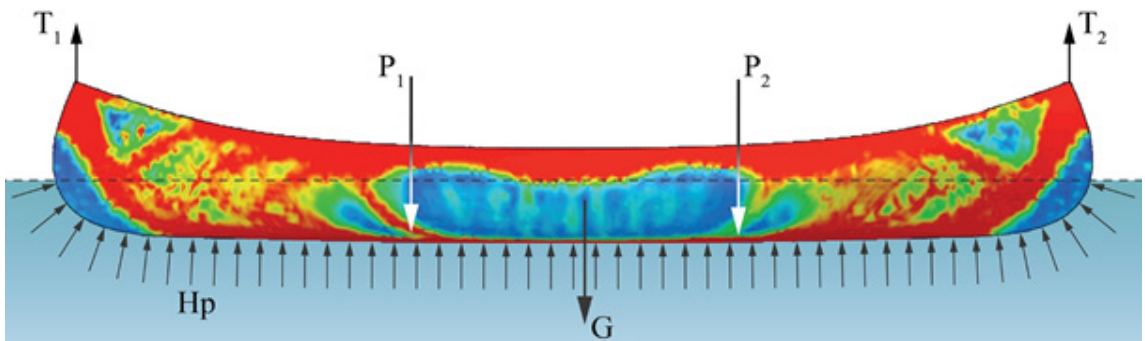


**Figure 3:** The two different load-cases used for the topology optimisation of the canoe: a) the floating load-case in water: self-weight ( $G$ ), live point loads from two canoeists ( $P_1$ ,  $P_2$ ), and a distributed support force provided by the hydrostatic pressure ( $H_p$ ); and b) a transport load-case on land: two support points ( $T_1$ ,  $T_2$ ) and self-weight.

**Source:** DBT, ETH Zürich, 2017

When designing a canoe, two aspects have to be considered: the structural integrity and waterproofing. Inspired by traditional wood and canvas canoes, these two functions are separated in two different construction layers:

a) The waterproofing of the canoe is ensured by a two-millimetre-thick outer “skin” made of highly fluid cement paste coated on cotton reinforcement. This process is described in-depth in a patent application and is not covered by this paper (Fontana et al., 2014).

b) The structural integrity is provided by an inner “skeleton” (Figure 4) which is fabricated using a 3D printed formwork, documented in this paper.

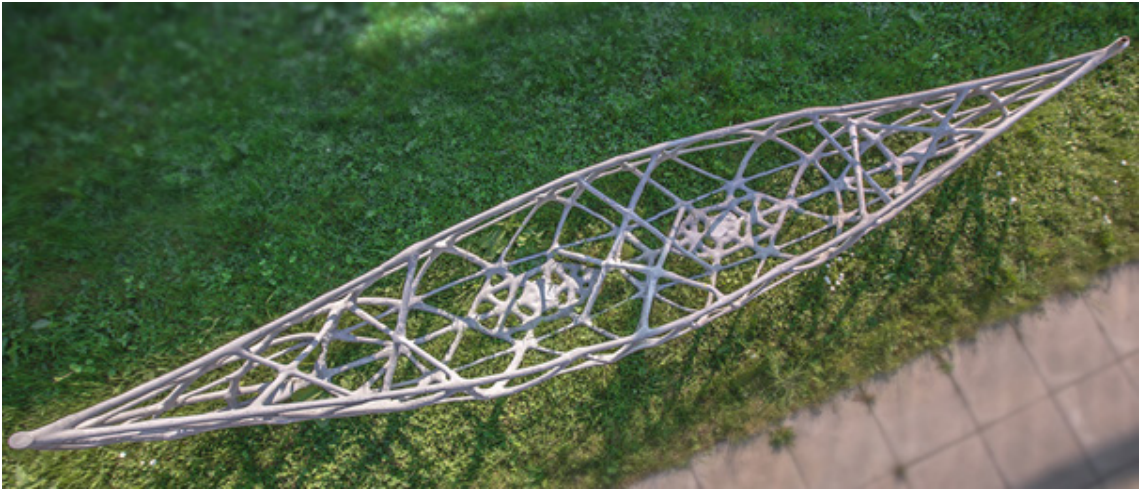


**Figure 4:** The complex concrete “skeleton” which provides the structural integrity for the canoe

**Source:** DBT, ETH Zürich, 2017

### Design through topology optimisation

Topology optimisation is an iterative computational process which determines the most efficient spatial configuration of material distribution in order to maximise certain performance criteria (Figure 5). The algorithm works within a confined, discretised space, with a set of given boundary conditions, i.e. loads and supports.

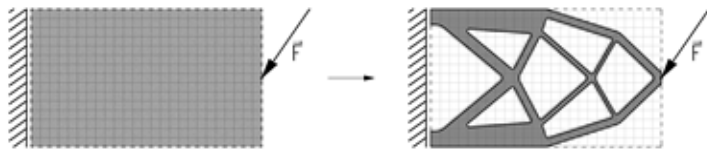


**Figure 5:** Sample topology optimisation of a simple rectangular design space with a single point load (left). After the topology optimisation, only 30% of the material is kept and distributed in order to minimise the deflection of the part (right).

**Source:** DBT, ETH Zürich, 2017

The starting point of the design was the outer shape of a traditional wood and canvas canoe for two persons. The 3D model was created based on its plan and elevation projections from a stock image (Figure 6). This solid volume containing two cavities for the canoeists served as the input solution space for the topology optimisation algorithm (Figure 7).

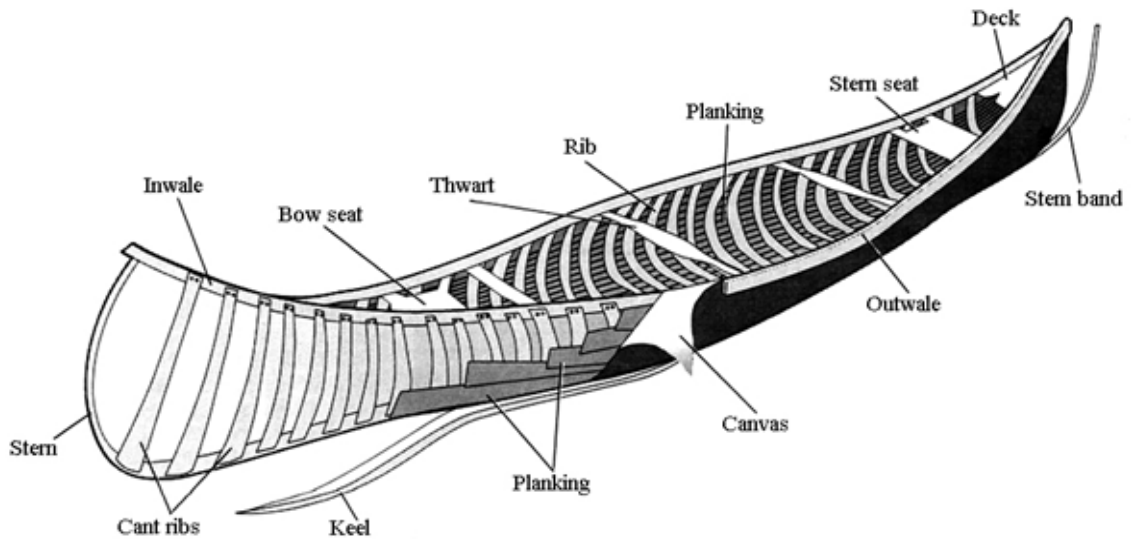


**Figure 6:** Traditional canoe shape used as starting point for the creation of the bounding volume. The structural skeleton of the concrete canoe is inspired by the ribs, keel and thwarts of the traditional canoe

**Source:** John Earle, The Virginia Beach Beacon

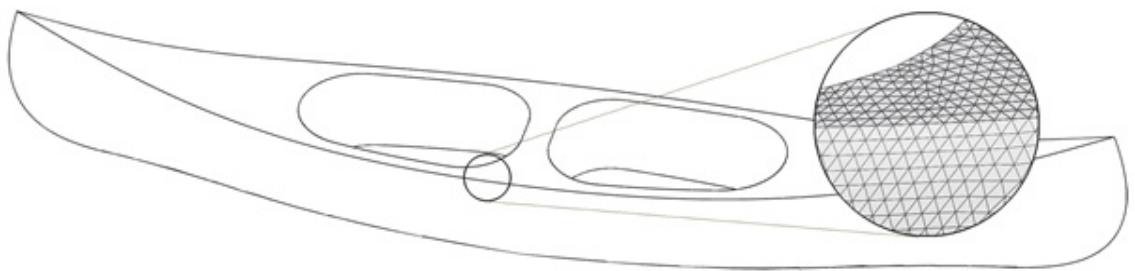


**Figure 7:** Bounding volume discretised into tetrahedral nodes of -15 mm edge length.

**Source:** DBT, ETH Zürich, 2017

For *skeLEThon*, the TOSCA engine of SIMULIA Abaqus was used to perform a simple topology optimisation. The design space was discretised into tetrahedral nodes of approximately 15 mm edge length. The supports and loads were defined for the two separate load cases as described above. The optimisation goals were to reduce material to a 0.15 set fraction of the initial volume while keeping to a minimum the strain energy of each node. The parameters used in the algorithm to describe the behaviour of concrete were a density of 2'400 Kg/m<sup>3</sup>, a Young's modulus of 50 GPa and a Poisson ratio of 0.2. The compressive and tensile strengths of concrete can be used in the engine to constrain the optimisation to safe results.

The result of a topology optimisation is the amount of strain energy and stresses calculated for every single node. When the predefined threshold of desired volume reduction is applied, a branching structure of ribs and tubes remains that optimally guides the forces through the structure. Some are explicitly present, others are only indicated by a gradient of porosity. This raw result serves as the input for the next step, where principal axes are retraced with a cage of NURBS curves, along crystallised, dense conglomerates of nodes.

At this stage, the axes can be adjusted slightly to tailor for any constraints of the fabrication process. In areas with lower density, additional auxiliary axes are introduced to limit the size of the open fields in the skeleton. This is because the waterproofing skin can only span over a limited surface, and whenever an opening is above this threshold, intermediary support is required (Figure 8).



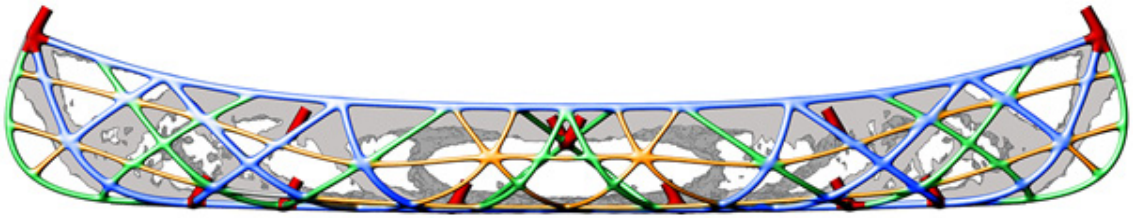


**Figure 8:** Elevation view of the structural skeleton. The initial solution space volume is reduced to the 15 % containing the nodes with the highest stress values (grey). Depending on these stress values, the resulting smooth bones have three different diameters: 35 mm (blue), 25 (green) and 15 mm (orange). Additional inlet and outlet tubes (red) are strategically added.

**Source:** DBT, ETH Zürich, 2017

This network of axes lines is then converted into the final formwork geometry of connected tubes by a custom volumetric modelling tool (Bernhard et al., 2018). Representing the bones as signed distance functions (FRep) is a very robust method. Complex topologies with different bone diameters meeting at acute angles are less prone to failure with FRep than with other methods based on explicit boundary representation (BRep) geometry. Depending on the amount of stress the bones take, they are classified in three different groups of 15, 25 and 35 mm diameter (Figure 8). After creating the entire skeleton of bones, a 3D Gaussian convolution kernel is applied to smoothen the sharp creases at the bone intersections and thereby improving both the concrete and the force flow (Figure 9).

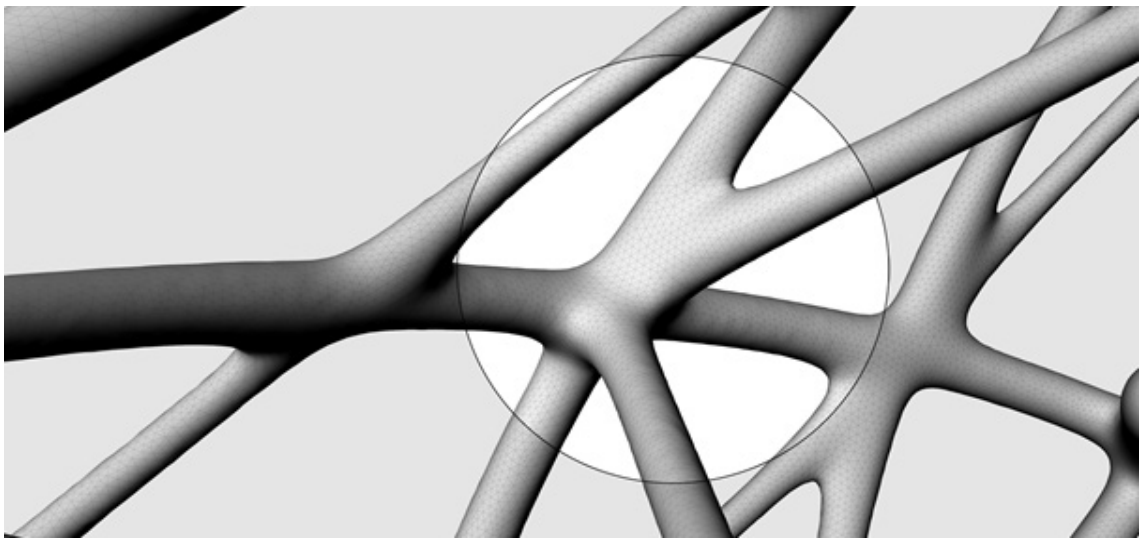


**Figure 9:** The intricate network of bones of the structural skeleton featuring complex spatial 3D nodes, with three to six bone edges coming together smoothly in order to create the thwarts of the canoe.

**Source:** DBT, ETH Zürich, 2017

### FDM 3D Printing

For the fabrication of the skeleton, FDM 3D printing was used first to produce the formwork. FDM is a widely available 3D printing technology in which molten material is extruded and hardens immediately after the deposition. The deposition progresses in consecutive horizontal layers which are generated as slices through a digital model of the part to be fabricated.

In particular, for *skeLETHon*, FDM was chosen because among the different 3D printing technologies, it is unique for its capability of producing large-scale and stable shells with thicknesses below 0.5 mm. Other 3D printing technologies are either capable of producing precise thin shells (such as selective laser sintering, stereolithography and certain metal 3D printing technologies) or have large printing volumes (like binder jetting),

but no other 3D printing method combines both large scale build volumes and the capacity to produce sub-millimetre shells. Moreover, the advantage of FDM is its accessibility, low cost and compatibility with a wide range of cheap plastics.

Out of this wide variety of plastics (biodegradable, water soluble, fibre-reinforced, flexible, conductive, low-shrinkage, bioplastics etc), translucent polylactic acid (PLA) was selected for the canoe. The choice was due to its versatility, low shrinkage factor, relatively good mechanical properties and environmentally-friendly pedigree (PLA is compostable, recyclable and based on renewable raw materials). Furthermore, PLA is relatively stable when exposed to environmental factors (humidity and temperature variations) and it can be 3D-printed in a wide domain of parameters, at temperatures between 180 and 240°C, with feed-rates of up to 300 mm/s.

FDM can resolve details with a precision of a tenth of a millimetre. This made possible the integration of a very fine functional surface texture on the formwork, in the range of 0.5 to 2 mm. This texture was introduced to increase the contact area and improve adherence between the skeleton and the waterproofing concrete layer (Figure 22).

Despite all its advantages however, FDM 3D printing also has a number of inherent limitations which are addressed by this research separately:

a) FDM is regarded as a slow fabrication process, usually able to produce volumetric flow-rates of 15 cm<sup>3</sup>/hour and resolve 0.1mm features. With well-tuned machines, flow-rates as high as 100 cm<sup>3</sup>/hour can be reached, but resolving power increases to 0.2 mm (i.e. less precision). The relatively slow speed of the 3D printing process is discussed in 2.4. Submillimetre Formwork for Concrete.

b) The limited amount of cantilever layers can reach in relation to each other (Figure 10). This is further discussed in 2.5. Formwork Fabrication.

c) The limited build volume of the 3D printers required a discretisation of the whole canoe in smaller parts which have to be assembled prior to casting. This limitation is further discussed in 2.6. Discretisation.

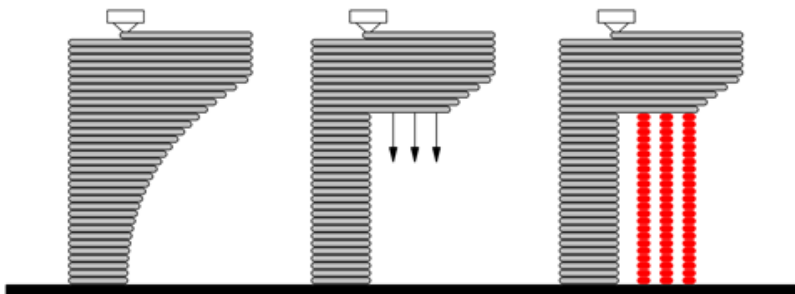


**Figure 10:** Fabrication limitations of FDM 3D printing. Below a certain threshold, horizontal layers can cantilever freely (left); Beyond this threshold, gravity would cause deformations and artefacts (middle); this can be resolved by introducing auxiliary support structures (in red, right). These support structures are mechanically removed or chemically dissolved at the end of the process

**Source:** DBT, ETH Zürich, 2017

In order to address the slow fabrication speeds, the unique capabilities of the FDM process were exploited to radically reduce the thickness of the formwork shell to submillimetre dimensions. For FDM technology, fabrication time is roughly directly proportional with the volume of the part. Therefore, by producing a very thin shell which is only 0.8 mm in thickness, the overall 3D printing volume was reduced to a minimum and this had a considerable impact on the overall printing time. By comparison, even the thinnest binder-jetted formworks are roughly ten times thicker (Jipa et al., 2016).

### Formwork Fabrication

Early fabrication tests have shown that in order to prevent 3D printing artefacts such as disconnected layers, over- or under-extrusion and local material deposits, the spatial orientation of the hollow formwork tubes had to be at least  $35^\circ$  as measured from a horizontal plane. This prevented the need to 3D print auxiliary support structures as described in Figure 10, which would have increased printing time unnecessarily. In order to suit this constraint, a shape optimisation step was performed following the topology optimisation, in which the angles of the tubes were adjusted to avoid very low inclinations (Figure 11).

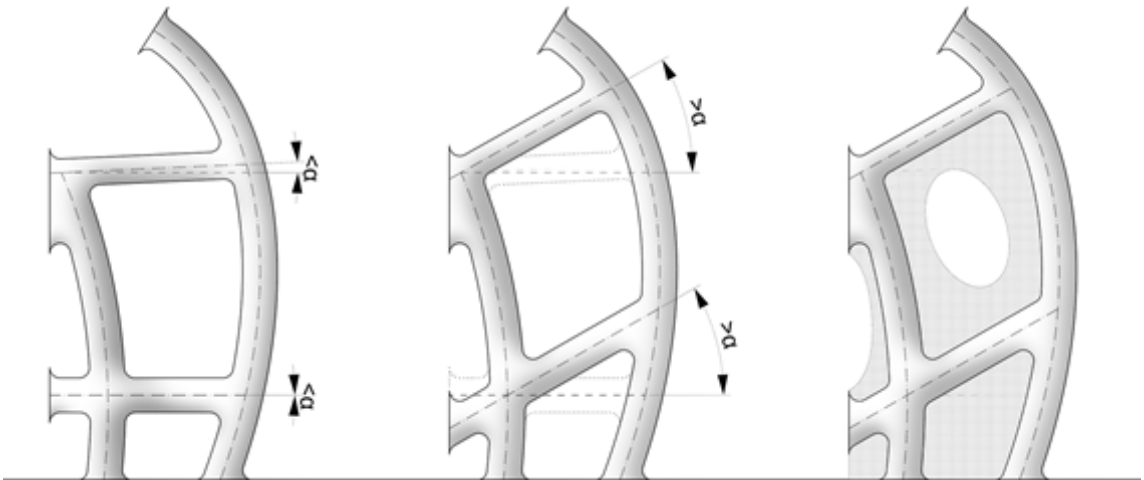


**Figure 11:** Diagrammatic section through a 3D printed part. In order to avoid auxiliary supports, the tubes are adjusted to achieve a minimal angle above an empirically determined threshold ( $\alpha > 35^\circ$ ). Lastly, membrane-like support structures are introduced to stabilise free-standing tubular structures (right).

**Source:** DBT, ETH Zürich, 2017

Another early empirical observation was that for taller parts, the movement of the gantry of the 3D printer caused vibrations which had a negative effect on the quality of tall and thin free-standing tubular parts. In order to prevent this, an auxiliary membrane-like support structure was parametrically introduced. This temporary support interconnects all the tubes in order to increase the stiffness of the part and reduce vibrations while printing (Figures 11, 12). Unlike a more conventional solid support system (Figure 10), these membranes did not bear the loads of the cantilevering layers, but only stiffened the free-standing geometric features in order to limit mechanically-induced vibrations. For reference, the membrane-like structures used for the *skeLETHon* formwork represent only about 6% of the volume of a conventional solid support system.



**Figure 12:** A 700-mm tall sample 3D printed part of the *skelETHon* formwork. In order to prevent quality issues for taller parts, a membrane-like auxiliary support structure is introduced.

**Source:** DBT, ETH Zürich, 2017

## Discretisation

Very large industrial FDM 3D printers exist, such as BigRep One, with a build volume above 1 m<sup>3</sup> and Big Area Additive Manufacturing with a volume of 5.8 m<sup>3</sup> (Post et al., 2016). However, for the canoe, only five basic entry-level consumer 3D printers were used. Four of them were Ultimaker Original+ 3D printers with build volumes of 210 × 210 × 205 mm. Two of these were modified with an extended vertical gantry, Z-Unlimited, commercialised by Rooieforis, to reach heights of up to 1 200 mm, for a total volume of 52.9 L each. The fifth 3D printer used was marginally larger, the Raise3D N2+, which has a build volume of 56.3 L (305 × 305 × 605 mm). While more robust 3D printing facilities would certainly benefit this method especially for larger scale architectural applications, the basic machines used for this project demonstrated the undemanding nature of the process and offered a good setup for investigating discretisation.

In order to address the limited volume of the 3D printers, the whole geometry was discretised in order to fit the print volume of the largest available printer. Thus, the formwork was split into 84 parts fitting 305 × 305 × 605 mm (Figure 13). Due to the two planes of symmetry of the boat, there were only 21 unique parts, plus their mirrored transformations.

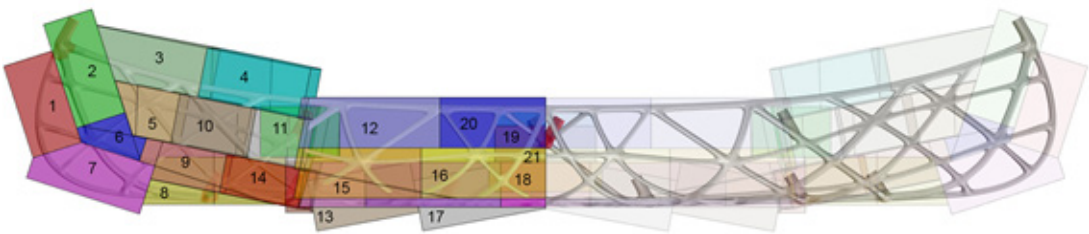


**Figure 13:** The 21 unique parts of the formwork which had to fit the maximum volume of the 3D printers.

**Source:** DBT, ETH Zürich, 2017

Due to the intricate differentiated geometry, the size of the parts varied considerably, with bounding box volumes between 3.1 L and 25.9 L. This opened the opportunity to use the smaller 3D printers for the smaller parts in order to distribute the fabrication time. Each part took between 4.5 hours for the smallest and 56 hours for the largest pieces, with an overall printing time of just under 1`000 hours.

Before casting the skeleton, the independent pieces had to be joined together (Figure 14). This was done through chemical welding with dichloromethane, which is an organic solvent for PLA. A 2 mm wide flange was integrated at each of the connections to provide a wider welding area. This detail is visible at the top of the component in Figure 12. The solvent is applied locally with a brush and dissolves the PLA on both sides of the connection. The dichloromethane is highly volatile and it evaporates in a few seconds, leaving a solid connection purely made out of PLA.

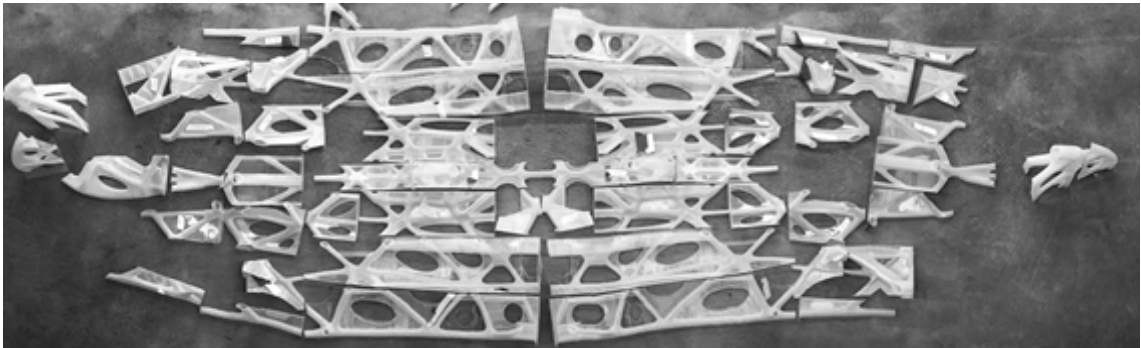


**Figure 14:** The 84 3D printed pieces before assembly.

**Source:** Moritz Studer, ETH Zürich, 2017

Finally, once the skeleton was assembled, a layer of transparent Polyester resin was applied on the surface in order to increase its stability for casting (Figure 15).



**Figure 15:** The 84 3D printed pieces assembled and ready for casting.

**Source:** DBT, ETH Zürich, 2017

### Concrete casting

For the casting process, ultra-high-performance concrete reinforced with ten-millimetre-long steel fibres (UHPFRC) was used (Ruffray et al., 2017). This satisfied the necessary rheological requirements for the concrete to flow through the very thin tubular geometric features of the canoe.

One of the critical issues related to concrete casting in submillimetre formwork is the build-up of hydrostatic pressure. The hydrostatic pressure ( $p_h$ ) is the maximum stress that is exerted uniformly by the fluid concrete on the formwork. Given a constant gravitational acceleration ( $g$ ), hydrostatic pressure is only dependent on the density ( $\rho$ ) of UHPFRC and the height ( $H$ ) of the fluid being cast, and it is independent of the diameter of the formwork tubes.

$$p_h = \rho g H \quad (1)$$

The very thin PLA formwork is unable to withstand the hydrostatic pressure of the dense UHPFRC used ( $\rho \sim 2 \cdot 400 \text{ Kg/m}^3$ ) for depths larger than  $\sim 100 \text{ mm}$ . The breaks in the formwork generally happen along the contact surface between consecutive 3D printed layers, where the tensile strength is lower due to the weak layer-to-layer interface.

In order to prevent the potential damages to the formwork caused by hydrostatic pressure, an auxiliary material was used to exert a counter-pressure on the formwork from the outside. To this effect, the canoe formwork was placed in a simple box (Figure 16) which was simultaneously being filled with sand while concrete was being cast inside the formwork (Figure 17). The level of concrete inside the formwork was synchronised with the level of the sand surrounding the formwork. Nevertheless, the density of sand ( $\rho \sim 1 \cdot 600 \text{ Kg/m}^3$ ) is lower than the density of UHPFRC, and therefore the sand counter-pressure does not entirely cancel the hydrostatic pressure of concrete out. However, it reduces it by about 70%, to a level where the thin plastic shell is stable enough.

Furthermore, the sand bed surrounding the formwork can also neutralise any potential breaks of the thin shell, by consolidating the formwork locally and preventing extensive concrete leaks.

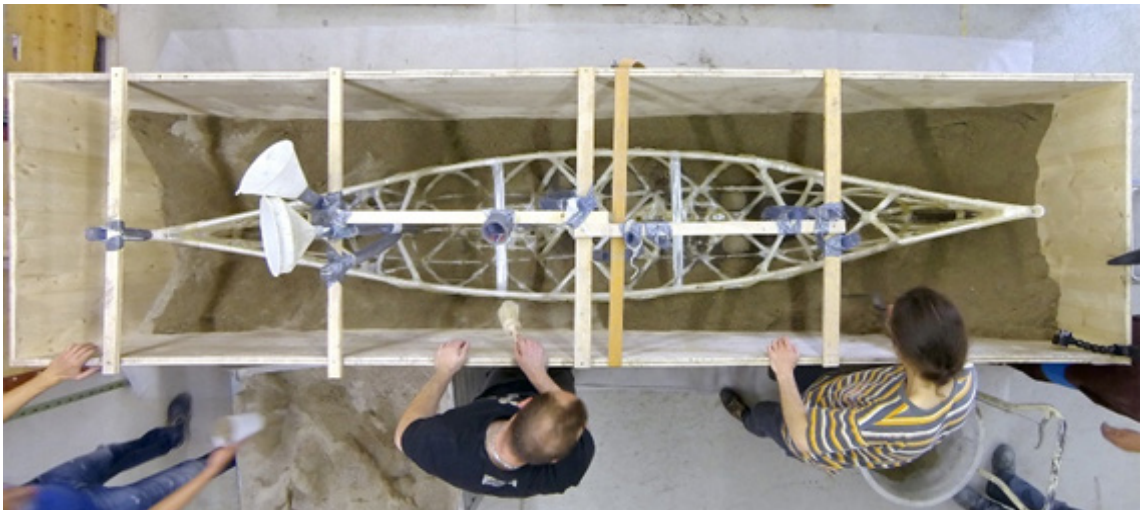


**Figure 16:** The canoe formwork was placed in a simple box which was simultaneously being filled with sand while concrete was being cast inside the formwork

**Source:** DBT, PCBM, ETH Zürich, 2017

The casting was initiated through inlets at the bottom of the formwork. This implies that the level of the concrete inside the shell rises uniformly. The transparent PLA formwork permits a visual inspection of the filling process to prevent air bubbles being trapped in complex nodes. As the concrete level reaches higher points, the sand bed on the outside is gradually filled to provide the necessary counter-pressure (Figure 17).

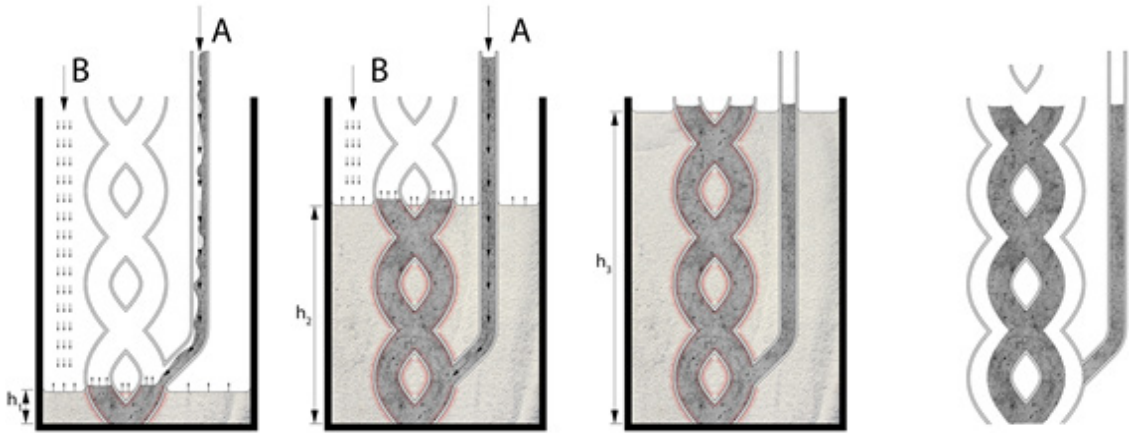


**Figure 17:** Step-by-step diagram showing the simultaneous infill of concrete through the bottom of the formwork (A) and of counter-pressure material (B). The final step consists of the removal of the formwork and casting inlet.

**Source:** DBT, ETH Zürich, 2017

One inlet point was however not enough for the entire canoe. The friction with the formwork walls accumulates and eventually overcomes the laminar flow of concrete once it travels a certain distance through the tubular network. In order to overcome this, ten inlet tubes were evenly distributed throughout the lower part of the canoe. At the highest points of the canoe, two further outlet points were provided in order to permit the air to evacuate the formwork. Air getting trapped inside the formwork is a significant risk, especially in horizontal tubes, where concrete flows in from both ends. Therefore, the canoe was tilted at an angle of 5° to the horizontal plane. This ensured that none of the tubes were perfectly horizontal and the concrete infill could be done progressively. Thus, the ten inlets were not used simultaneously from the beginning, but rather in a sequence, whenever the concrete level would reach their corresponding infill point (Figure 18).

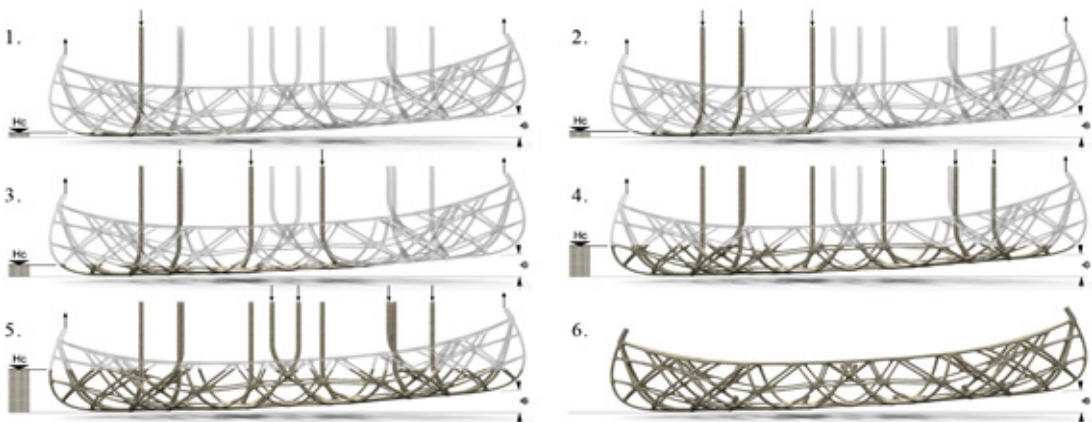


**Figure 18:** The casting sequence of the concrete canoe. The ten inlet points are situated at different heights in the lower part of the formwork. Casting starts through the lowest inlet point (1). The level of concrete inside the formwork ( $H_c$ ) raises gradually. Higher inlet points are used progressively as  $H_c$  increases (2-5). Once the entire canoe is filled, the inlet tubes are removed mechanically (6).

**Source:** DBT, ETH Zürich, 2017

Following the concrete casting, the PLA formwork provides the perfect enclosure for concrete curing, preventing cracking due to water loss. After curing for seven days, a heat-gun was used to supply moderate heat (~200°C) and the formwork can be peeled off (Figure 19).

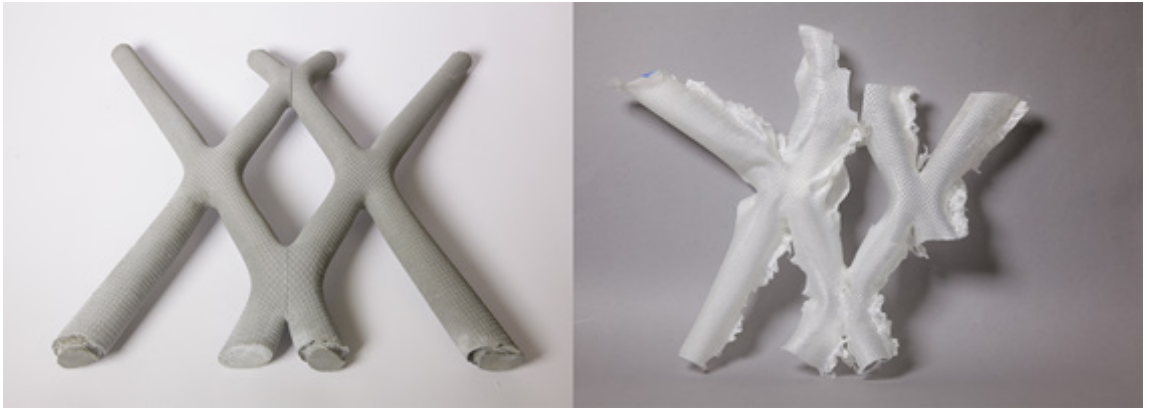


**Figure 19:** UHPFRC prototype (left) after the removal of the submillimetre formwork (right).

**Source:** DBT, ETH Zürich, 2017

## Discussion

At the 16th Concrete Canoe Regatta (Figure 20), *skelETHon* received the first prize for design innovation, being commended for the ingenious use of digital fabrication to indirectly produce the intricate concrete skeleton structure. The design and fabrication process of this canoe highlighted the harmonious compatibility between the additive digital fabrication process and the topology optimisation used for form-finding purposes.



**Figure 20:** *skelETHon* at the 16th Concrete Canoe Regatta in Cologne, Germany

**Source:** DBT, ETH Zürich, 2017

The key achievement was to keep the thickness of the formwork in the 0.6 to 1 mm range in order to minimise material use and keep fabrication time to a minimum. This was made possible by the unique properties of FDM 3D printing. The relatively expensive and time-consuming 3D printing process is only used for the very thin shell which defines the shape. This is possible because most of the structural stability of the formwork during casting is provided by the sand bed surrounding the formwork.

Such an extreme reduction in the thickness of the formwork has further implications:

a) It minimises tolerances and maximises dimensional accuracy due to reduced thermal shrinkage. For a given temperature variation, the linear and volumetric thermal shrinkage are a fixed percentage of the initial length and volume respectively. For PLA cooling down to room temperature after 3D printing, the linear shrinkage is ~0.25 to 0.3 %. Thus, a 0.8 mm shell will only shrink ~2  $\mu\text{m}$ .



b) Without any release agents and postprocessing steps, the plastic formwork is easily removable.

c) Reduced labour and stream-lined construction process: faster off-site fabrication time for the formwork, reduced cost of transportation to site and easier on-site manipulation and assembly.

d) Considerable formwork material reduction and lower embodied energy for concrete construction overall, given the significant proportion of resources that the formwork represents in conventional concrete constructions. For reference, a commercial lightweight formwork system needs around 30 Kg of formwork / 1 m<sup>2</sup> of concrete, while for the canoe, only 1 Kg / m<sup>2</sup> were necessary (5.5 Kg of PLA formwork for 5.5 m<sup>2</sup> of concrete). The robustness of the proposed system is naturally very low by comparison, but this is addressed in the next chapter, *2.5 Formwork Fabrication*.

Reducing the amount of formwork to a minimum also keeps the costs of the formwork low. For the canoe, the formwork represented roughly twice the cost of the concrete. This is twice as much as the cost of standard formwork in a conventional concrete component. Nevertheless, the canoe had a much larger specific formwork surface area (157 m<sup>2</sup> of formwork / m<sup>3</sup> of concrete) compared to a standard project (2-5 m<sup>2</sup> of formwork / m<sup>3</sup> of concrete). Moreover, compared to the cost of the 3D printed formwork for the canoe, a bespoke commercial formwork system costs roughly 50 times more per m<sup>2</sup>. At this point, there is insufficient data to draw a conclusive direct comparison between 3D printed formwork and a standard system. Nevertheless, the numbers suggest that for bespoke, one-of-a-kind geometries, 3D-printed formwork can offer significantly lower costs, despite the early development stages of the technology.

Freeing the 3D printed shell from the need to provide stability, also allowed an unprecedented geometric freedom to be possible with concrete. Due to the topology optimisation algorithm used in the design, concrete was used in a very efficient way, with bones of various thicknesses being optimally distributed to provide maximum stiffness for the frame (Figure 21). The skeleton weighed just under 80 Kg, while the final weight, including the waterproofing layer was 114 Kg. Such an intricate topology, with unique spatial nodes where between three and six linear elements meet at custom angles (Figure 9), with various degrees of smoothness, would be otherwise impossible to fabricate with any other production process.

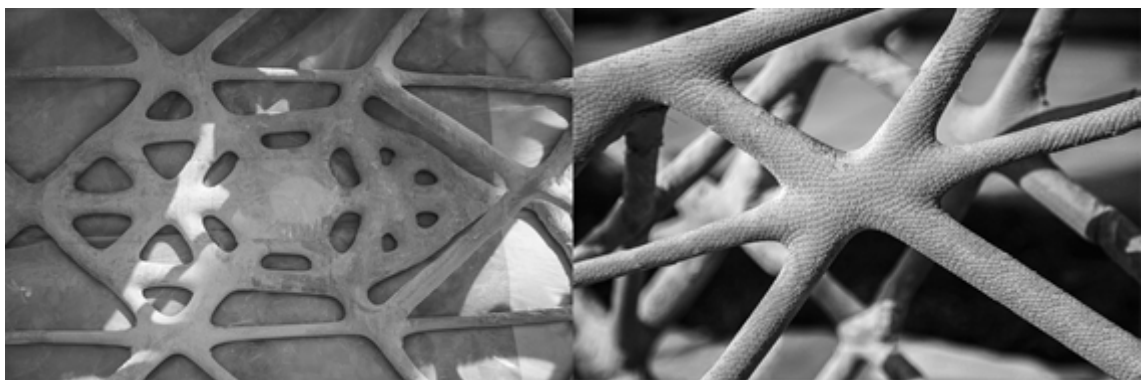


**Figure 21:** A wide range of geometric features resulted from the topology optimisation algorithm, with denser areas occurring on the keel, where the point loads from the canoeists are concentrated (left); and more open nodes on the hull, where only distributed loads are present (right)

**Source:** DBT, ETH Zürich, 2017

Another key achievement was to transfer faithfully a sub-millimetre surface texture from the 3D printed formwork to the concrete (Figure 22). This texture maximises the contact area with the waterproofing skin. Extrapolating this capability to architecture, these fine and precise surface treatments could fulfil other roles, such as acoustic diffusion, haptics or ornamentation for structural building elements.

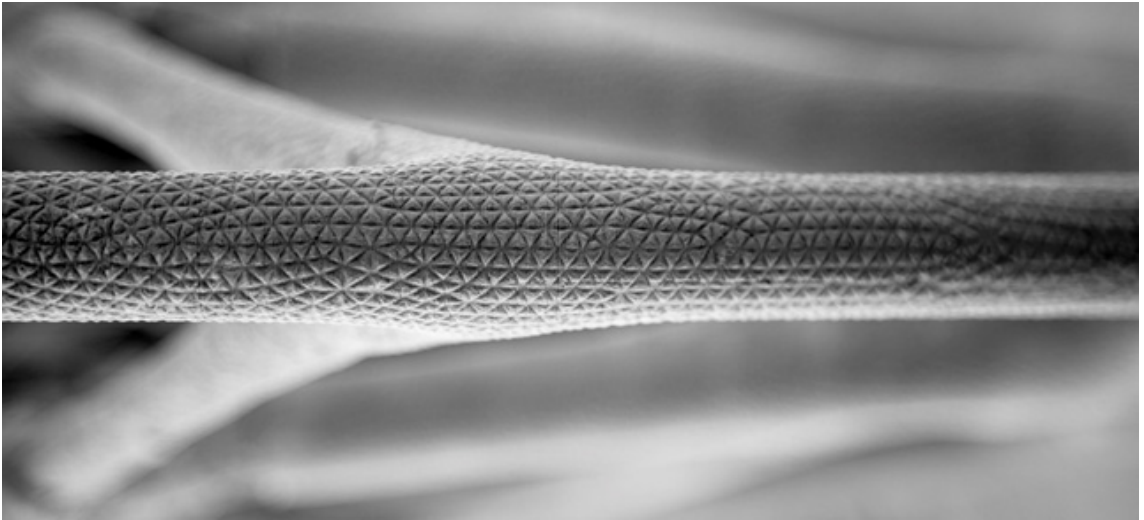


**Figure 22:** High resolution texture on the surface of stern and inwale of the *skelETHon*. This texture maximises the contact area with the waterproofing concrete skin.

**Source:** DBT, ETH Zürich, 2017

Such a high-resolution texture would otherwise be challenging and time-consuming to achieve with subtractive processes like milling or hot wire cutting. While not unlimited, the geometric freedom offered by FDM certainly complements the other digital fabrication processes available for making formwork. A single fabrication process able to produce any geometry in large scale is not available at the moment, but FDM can be a very efficient tool in producing highly specialised geometries, such as networks of tubes and thin shells, impossible to fabricate otherwise.

## Outlook

The canoe also highlighted a number of areas which can be addressed by future research in order to make this method suitable for streamlined large scale production:

a) The speed and reliability of the 3D printing process often caused issues, mostly related to the specific type of hardware used. An FDM machine with multiple hot ends, optimised for sustained printing in large volumes would greatly benefit this research.

b) The stability of the formwork can still be problematic at welding points. This is partly due to the large number of parts in which the formwork had to be discretised as a consequence of the small 3D printers used. 3D printing tolerances accumulate in the welding process and cause weaknesses. These weaknesses can lead to leaks of concrete during the casting process. While the sand bed quickly neutralises the leaks, the consistency of the formwork fabrication has to be addressed.

c) Partly due to these inconsistencies, the current process is fundamentally suitable for off-site prefabrication of construction elements. The nature of the casting process where the concrete infilling has to be correlated with the sand-bed counter-pressure is only suitable in a controlled environment. This is because the concrete infill does not happen uniformly as initially predicted. Due to the variable friction with the formwork, wider tubes get filled up faster than narrow ones, which causes different concrete levels at different areas of the formwork. In order to overcome this issue, computational fluid dynamics simulations could be used to design a strategy for positioning inlets as well as adjust the diameters of the formwork tubes in order to ensure a predictable level of concrete throughout the casting process.

d) Another type of simulation that could potentially give valuable insight into this process would be the analysis of the behaviour of the steel fibre reinforcement in such a tubular structure, especially around complex nodes. The consistent orientation of the fibres is critical in ensuring the bending strength of concrete, but the behaviour of the fibres throughout the casting process is difficult to anticipate intuitively. Combined with an empirical method such as X-ray computed tomography (CT) scanning of physical prototypes this could inform the geometry of such skeletons in a meaningful way (Figure 23).

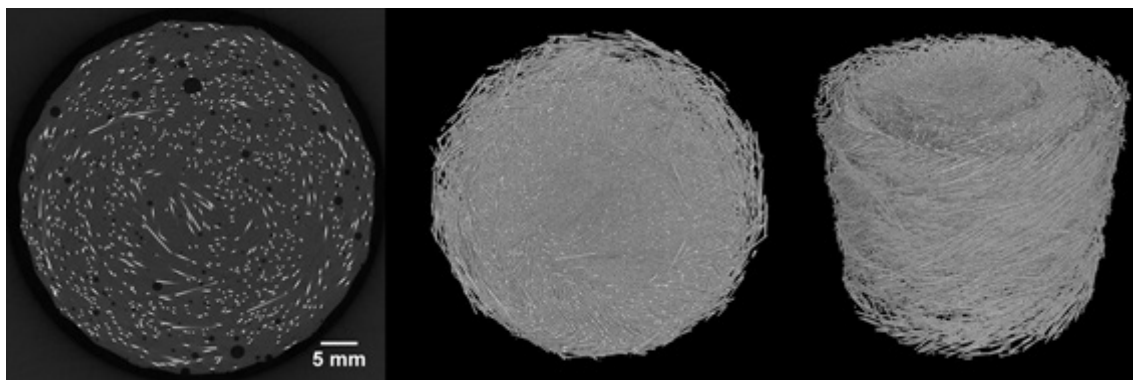


**Figure 23:** Preliminary CT scan of a concrete tube, showing the distribution and orientation of the steel fibre reinforcement, as well as air bubble inclusions.

**Source:** Michele Griffa, EMPA, Dübendorf, Switzerland

### Conclusion

The fabrication process tested with the canoe shows how a cutting-edge digital fabrication technology can be used minimally to fabricate a thin shell formwork which accurately defines the shape, while the stability of the formwork is transferred to a common secondary material, such as sand. The gradual sand filling process, combined with the transparency of the formwork allow live feedback on the casting process, which is critical for intricate geometries.

This novel process can be extrapolated and directly adapted for the design and prefabrication of large, load-bearing, concrete architectural components. The size of the canoe, approximately  $4 \times 0.7 \times 0.7$  m is representative for a building component such as a column, a beam or a façade element and the infrastructure necessary for the casting (i.e. containers for sand) is easily available. The key achievements demonstrated with the canoe can make a big difference on the way concrete is used in architecture: almost unconstrained geometric freedom, significant weight reduction, lightweight formwork and high precision for on-site assembly.

The complexity of the formworks possible, combined with the excellent rheological properties of UHPFRC open up an entirely new family of shapes for concrete building elements: microstructures, free form surfaces, highly detailed textures, precise articulations and convoluted topologies.

With 3D printing, each fabricated part can be unique, since the manufacturing process does not involve the use of expensive moulds which need to be re-used to make them cost-effective. 3D printing one-of-a-kind pieces of formwork, for customised concrete elements specifically tailored for their individual purpose is therefore possible, with no cost or time penalties. These are the first steps towards the mass-customisation of buildings through non-standard, prefabricated concrete components which integrate structural, functional and aesthetic solutions, as well as additional features such as weight reduction and a smart assembly logic.

## Acknowledgments

The authors would like to thank a number of partners and collaborators whose dedication was essential for this research:

- Heinz Richner and Andi Reusser (Concrete Lab, D-BAUG, ETH Zürich);
- Moritz Studer, Oliver Wach, Kathrin Ziegler (Civil Engineering bachelor students, ETH Zürich);
- Matthias Leschok, Ioannis Fousekis (DBT, Student Assistants);
- Lex Reiter (PCBM, IfB, D-Baug, ETH Zürich);
- The Concrete Canoe Club Zürich (Pirmin Scherer, Lukas Fuhrmann, Hannes Heller, Patrick Felder, Jonas Wydler, Jonas Henken, Andreas Näsdom, Anna Menasce, Caterina Rovati, Roman Wüst, Pascal Sutter, Thomas Rupper, Jonathan Hacker);
- Sika AG, Holcim, Allplan, RooieJoris, Specht-Technik, German RepRap (Concrete canoe sponsors);

This research was supported by the NCCR Digital Fabrication, funded by the Swiss National Science Foundation (NCCR Digital Fabrication Agreement #51NF40-141853).

## REFERENCES

- Aghaei-Meibodi, M., Bernhard, M., Jipa, A., & Dillenburger, B. (2017). The Smart Takes from the Strong. *Fabricate 2017: Rethinking Design and Construction*.
- Amir, O. (2013). A topology optimization procedure for reinforced concrete structures. *Computers & Structures*, 114, 46–58. Elsevier.
- Bernhard, Mathias, Michael Hansmeyer, & Benjamin Dillenburger. (2018). Volumetric Modelling for 3D Printed Architecture. *AAG 2018, Advances in Architectural Geometry 2018*, 392–415. Klein Publishing GmbH.
- Crow, J. M. (2008). The concrete conundrum. *Chemistry World*, 5(3), 62–66.
- Fontana, M., Flatt, R., Marchon, D., & Lex, R. (2014). Switzerland Patent No. EP 2 902 183 A1. E. P. Office.
- Hack, N., Lauer, W., Langenberg, S., Gramazio, F., & Kohler, M. (2013). Overcoming Repetition: Robotic fabrication processes at a large scale. *International Journal of Architectural Computing*, 11(3), 285–299. SAGE journals.
- Hack, N., & Lauer, W. V. (2014). Mesh-Mould: Robotically Fabricated Spatial Meshes as Reinforced Concrete Formwork. *Architectural Design*, 84(3), 44–53. John Wiley & Sons Ltd.
- Gardiner, J. B., & Janssen, S. R. (2014). FreeFAB - Development of a Construction-Scale Robotic Formwork 3D Printer. *Robotic Fabrication in Architecture, Art and Design 2014* (pp. 131–146). Springer.
- Jipa, A., Bernhard, M., Dillenburger, B., & Aghaei-Meibodi, M. (2016). 3D-Printed Stay-in-Place Formwork for Topologically Optimised Concrete Slabs. *TxA Emerging Design + Technology*. Kory Bieg.
- Jipa, A., Bernhard, M., & Dillenburger, B. (2017). Submillimeter Formwork. 3D Printed Plastic Formwork for Concrete Elements. *TxA Emerging Design + Technology* (p. 9). Kory Bieg.
- Kaczynski, M. P. (2013). Crease, Fold, Pour: Rethinking flexible formwork with digital fabrication and origami folding. *ACADIA 2013: Adaptive Architecture*.
- Lloret, E., Shahab, A. R., Linus, M., Flatt, R. J., Gramazio, F., Kohler, M., & Langenberg, S. (2015). Complex concrete structures: Merging existing casting techniques with digital fabrication. *Computer-Aided Design*, 60, 40–49. Elsevier.
- Morel P., Schwartz T. (2015). Automated Casting Systems for Spatial Concrete Lattices. *Modelling Behaviour*. Springer, Cham.

Nervi, P. L. (1956). Structures. FW Dodge Corp.

Oesterle, S., Vansteenkiste, A., & Mirjan, A. (2012). Zero waste free-form formwork. International Conference on Flexible Formwork, ICFE.

Peters, B. (2014). Additive Formwork: 3D Printed Flexible Formwork. ACADIA 14: Design Agency.

Popescu, M., Reiter, L., Liew, A., Van Mele, T., Flatt, R. J., & Block, P. (2018). Building in Concrete with an Ultra-lightweight Knitted Stay-in-place Formwork: Prototype of a Concrete Shell Bridge. Structures, 14, 322-332. Elsevier.

Post, B., Lloyd, P. D., Lindahl, J., Lind, R. F., Love, L. J., & Kunc, V. (2016). The Economics of Big Area Additive Manufacturing: Oak Ridge National Laboratory (ORNL). Manufacturing Demonstration Facility (MDF). Oak Ridge.

Robert, H. (2007). Think formwork-reduce cost. Structures, 14. Elsevier.

Ruffray, N., Bernhard, M., Jipa, A., Aghaei-Meibodi, M., Taisne, N. M. d., Stutz, F., Wangler, T., Flatt, R., & Dillenburger, B. (2017). Complex architectural elements from HPFRC and 3D printed sandstone. Symposium on Ultra-High Performance Fibre-Reinforced Concrete. RILEM.

Rust, R., Jenny, D., Gramazio, F., & Kohler, M. (2016). Spatial Wire Cutting: Cooperative robotic cutting of non-ruled surface geometries for bespoke building components. CAADRIA: Living Systems and Micro-Utopias: Towards Continuous Designing.

Søndergaard, A., & Dombernowsky, P. (2011). Unikabeton prototype. Fabricate 2011: Making Digital Architecture.

Veenendaal, D., West, M., & Block, P. (2011). History and overview of fabric formwork: using fabrics for concrete casting. Structural Concrete, 12(3), 164-177. John Wiley & Sons Ltd.

**Andrei Jipa**

jipa@arch.ethz.ch

**Mathias Bernhard**

bernhard@arch.ethz.ch

**Nicolas Ruffray**

nicolas.ruffray@ifb.baug.ethz.ch

**Dr. Timothy Wangler**

wangler@ifb.baug.ethz.ch

**Prof. Dr. Robert Flatt**

flattr@ethz.ch

**Prof. Dr. Benjamin Dillenburger**

dillenburger@arch.ethz.ch